LHCb note 99-009
23 May 1999

Signal observation from minimum ionizing particles and time resolution estimation in the Triple-GEM detector

B.Bochin, V.Gromov, A.Kashchuk*, V.Poliakov
Petersburg Nuclear Physics Institute of the Russian Academy of Sciences

Abstract

Recently a Triple-GEM detector constructed at PNPI has been tested in a PSI hadronic beam (π+ pions at 215 MeV/c and protons at 350 MeV/c). GEM-foils used in the detector have a pitch of 140 μm and Kapton hole size of about 40 μm. The detector has a sensitive area of 100×100 mm^2 and a 2 mm drift gap. The anode plane contains strips with 300 μm pitch. The detector was operated with the mixture of 0.7Ar+0.3CO$_2$ at a gas gain about 1×10^4. It has shown good operation reliability in high intensity hadron beams up to 3×10^6 Hz/cm^2. Signals from both sides of the induction gap, i.e. from the GEM and from the anode strips, have been recorded with the wide-band digital scope. The current pulses produced by MIPs in the detector have been reconstructed. The time resolution of the Triple-GEM detector has been estimated from the recorded data: rms≈6ns.

1. Experimental setup

Fig.1 shows the experimental setup. Counters S1 and S2 in coincidence with a mini-scintillator S3 (1×5×40mm^3) were used to trigger the digital scope recording signals from the GEM-detector.

A π+beam at 215 MeV/c with a rate of ≈30 kHz/cm^2 was used normally in the measurements. However, there were runs with a proton beam at 350 MeV/c with rate ≈3 MHz/cm^2.

The Triple-GEM detector was set on a moveable table. It was powered from two HV supplies with negative polarities. One supply (CAEN, Mod.N471A) was connected to the cathode (V1) and the second one (NHQ, 226L) was connected to the resistive divider (V2). The divider supplied HV to all the other elements: GEM1, GEM2, GEM3 (Fig.2). The HV was controlled from the counting room. Discharges in the detector could be detected either as increasing current in the first power supply or with the digital scope.

Only three channels from neighbouring strips (i-1, i, i+1) were analysed in these measurements with the digital scope. Also, the GEM3 foil from the induction gap side was connected to the so called 'Common Channel Amplifier' through a decoupling capacitor, as shown in Fig.2. Thus, four lines were transported over 25 meters with 50 Ohm cables from the experimental area into the counting room. The cables were connected to the 4-channel digital sampling oscilloscope (Tektronix TDS 654C, 500 MHz, 5GS/s). The scope was triggered by either scintillator counters (with Trigger logic) or by one of the selected channels. The scope was linked to a PC for recording data into the files.

* corresponding author 'kashchuk@hep486.pnpi.spb.ru'

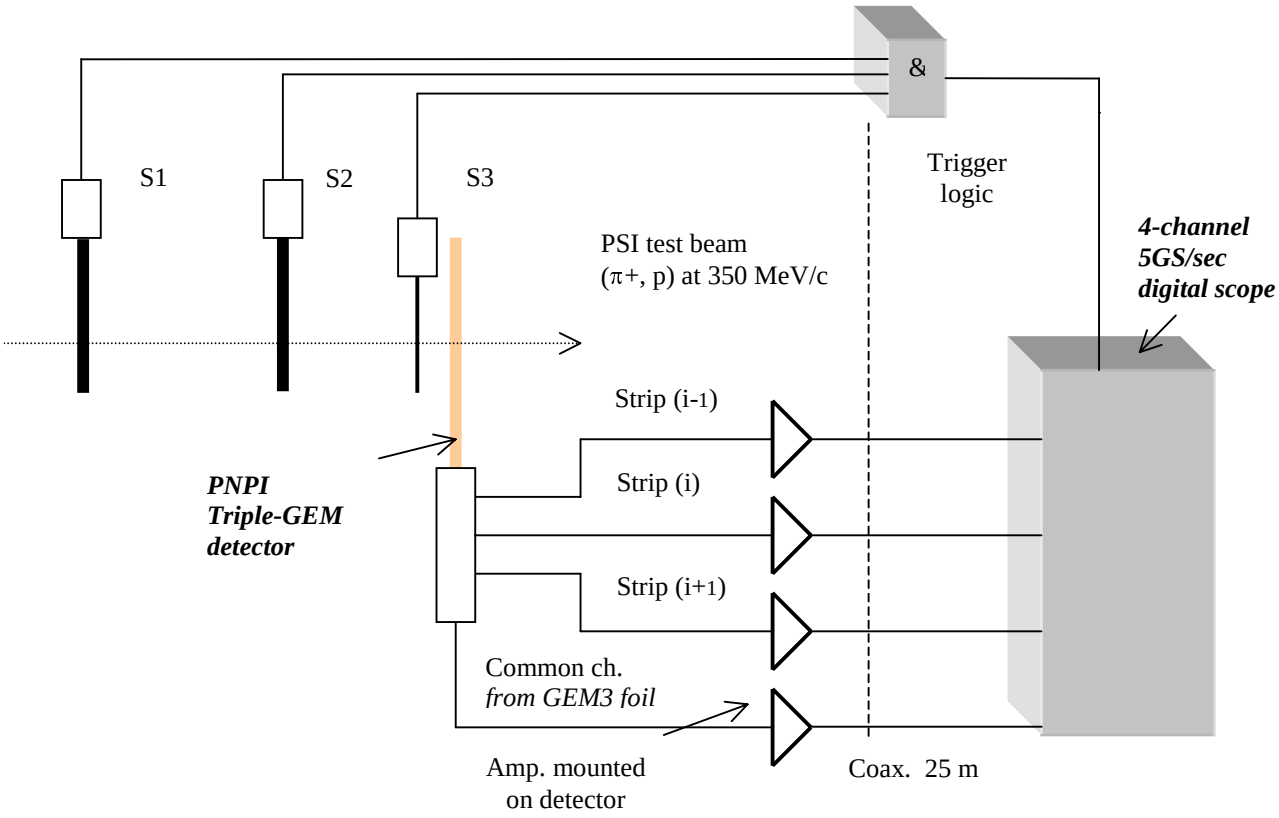

Fig.1. Experimental set-up.
S1, S3 - beam counters; S2 – mini-scintillator (1×5×40mm^3).

2. Triple-GEM detector

The Triple-GEM detector tested in the PSI hadronic beam has been redesigned with respect to the previous one /1,2/. Fig.2 shows the schematic view of the new detector.

The GEM-foils were made at CERN on 50 μm Kapton coated with Cr+Cu+Ni+Au (5 μm total thickness) with the active size of 100×100 mm^2. The shape of each hole in the GEM-foils is symmetrically conical with diameters of 80/40/80 μm (metal/dielectric/metal).

The cathode and the anode of the Triple-GEM detector were made of RF4 plates 100 μm thick. On one side the plates were coated with 5 μm of copper. The anode contained 150 μm strips with 300 μm pitch.

All detector planes were separated with 2 mm spacers and were assembled in the closed gas volume. The volume had one gas inlet and one gas outlet for connection to the gas system with a 6mm Swagelok connector. The spacers had some holes to allow free gas flow inside the chamber.

The connections of the electrodes to the divider and the strips to the amplifiers (Fig.3) were made outside the gas volume through sockets hermetically mounted in the walls of the chamber.

The active area of this Triple-GEM detector had a radiation thickness of about 0.75%X_0.

3. Results of measurements

Fig. 4 shows the effective gas gain of the Triple–GEM detector at various V2 at fixed V1=-3.0kV. This curve was measured before and after the irradiation of the detector in the PSI beam. No visible difference was found. The detector was operated with the gas mixture $0.7Ar+0.3CO_2$ at an effective gas gain of about 1×10^4. The variation of the gas gain over the active area of the detector was ±20%.

The first stage of the amplifier used in the measurements (Fig.3) is the PNPI hybrid charge-sensitive preamplifier with Cf=3.7pF and Rf=16kOhm (gain about 0.2mV/fC, RfCf=60ns). The next two stages are the fast voltage amplifiers (gain is equal to 6 per stage). The pulse response function of the amplifier (falling edge time constant of 60 ns) are shown in Fig.5 at $C_{det}\approx40$pF and in Fig.6 at $C_{det}=C_{strip}$. The total sensitivity of the amplifier was about 1.6 mV/fC including an attenuation and an integration of the analysed signals in the cables.

Fig.7*(b)*, 8*(b)* and 9*(b)* show the signals recorded by the digital scope (polarities of the signals have been inverted by the scope). Using the fit of the pulse response function of the amplifier (Fig.5 and Fig.6), the current pulses from the Triple-GEM detector were reconstructed. One can see rather good agreement between the data measured and calculated. Fig.7*(a)* shows the current pulse in the GEM from the induction gap (common channel). It is constant during the induction of the charge moving through the induction gap. The width of the pulse corresponds to the drift velocity of the electrons in the drift gap.

Fig.8*(a)* shows the current pulse in the central strip of the hit cluster. It has in the base the same width as the previous pulse, but it consists of two components: a tail at the front followed by a fast component. The tail corresponds to the induction of the moving charge from a large distance, and the fast component corresponds to the induction of the moving charge close to the strip. Fig.9*(a)* shows the current pulse shape in the neighbouring strip. Its total width matches the width of the pulse in the central strip, but it also consists of two parts. The first part corresponds to the tail, i.e. to induction from a large distance, and the second one develops in time when the moving charge is collected in the central strip.

The time resolution of the Triple-GEM detector has been estimated from the recorded data at V1=-3 kV and V2=-2.8 kV ($I_{divider}$=189μA). The electric fields in the gaps were as follows: Edrift=2.95 kV/cm; $E_{transport}$=2.26 kV/cm; $E_{induction}$=2.84 kV/cm. Fig.10 shows a distribution of the peaking time of pulses on the central strip from which the time resolution has been found to be rms=6.5 ns. The time resolution measured in the common channel is equal to rms≈6ns. These results are in a good agreement with the time resolution obtained for the Double-GEM detector in ref./3/ for the same gas mixture (FWHM≈17ns).

In conclusion, the reconstructed current pulses produced by MIPs in the Triple-GEM detector give us the possibility of optimizing the front-end electronics for future measurements.

Acknowledgements

The authors thank A.A.Vorobyov and U.Straumann for their continuous support of work and F.Sauli for useful discussions. We acknowledge also A.Zdanov for the mini-scintillator, A.Gandi and R.Lindner for the GEM foils. Also we want to thank very much our Heidelberg and Zurich colleagues, who made the infrastructure available for us during tests.

***Reference*s**

1.B.Bochin, A.Kashchuk, V.Poliakov.
Preprint PNPI-2283, 1998, Petersburg Nuclear Physics Institute, Gatchina.
2.B.Bochin, A.Kashchuk, V.Poliakov, A.A.Vorobyov.
LHCb note 98-068, 30 December 1998.
3.A.Bressan, J.C.Labbe, P.Pagano, L.Ropelewski, F.Sauli.
Nucl.Instrum.Methods Phys.Res., A425 (1999), 262-267.

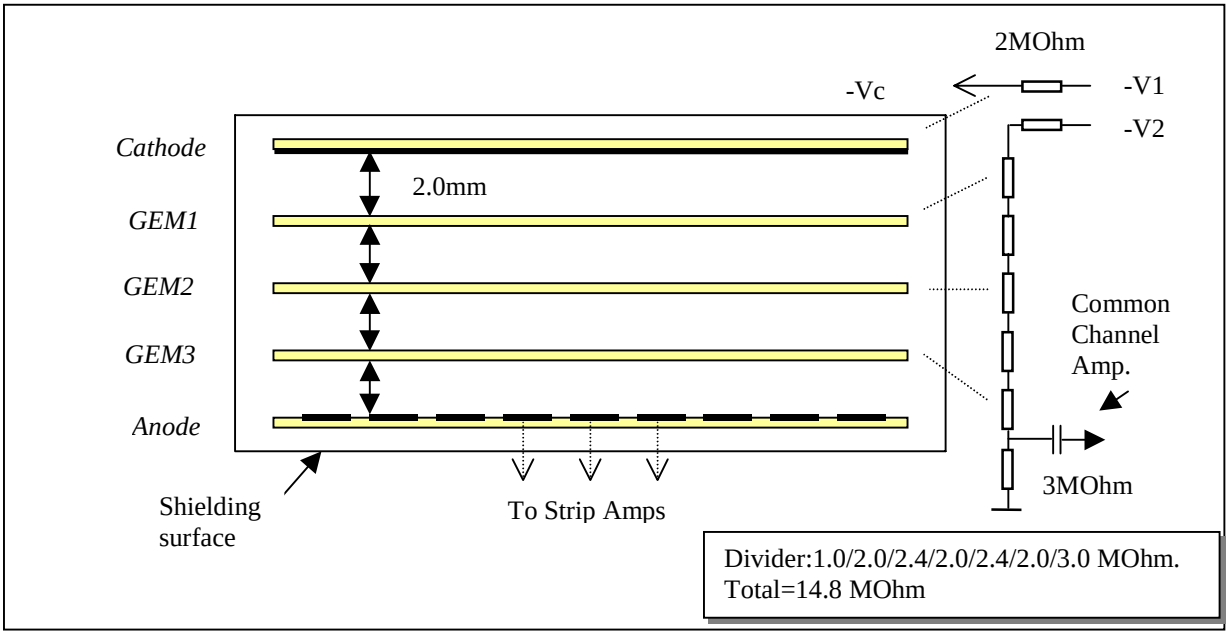

Fig.2. Schematic view of the Triple-GEM detector.

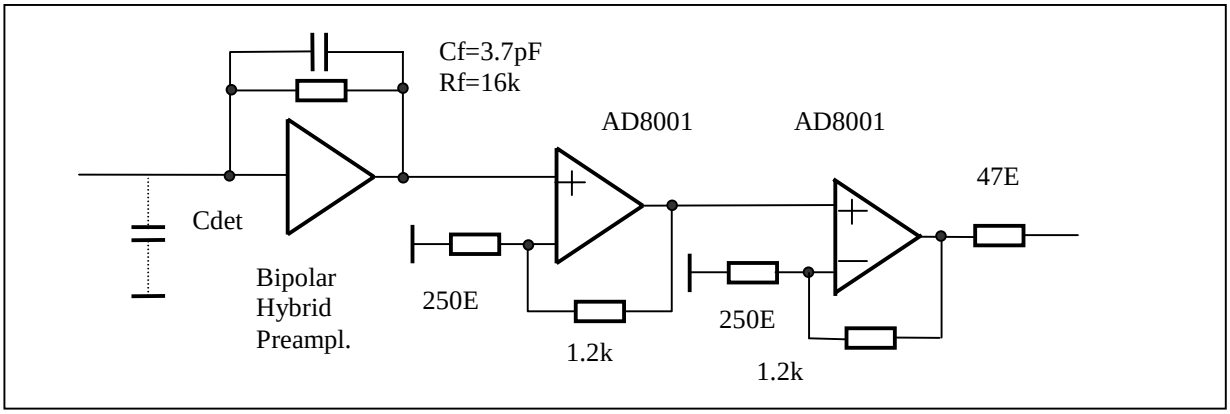

Fig.3. Scheme of the amplifier used in the measurements.

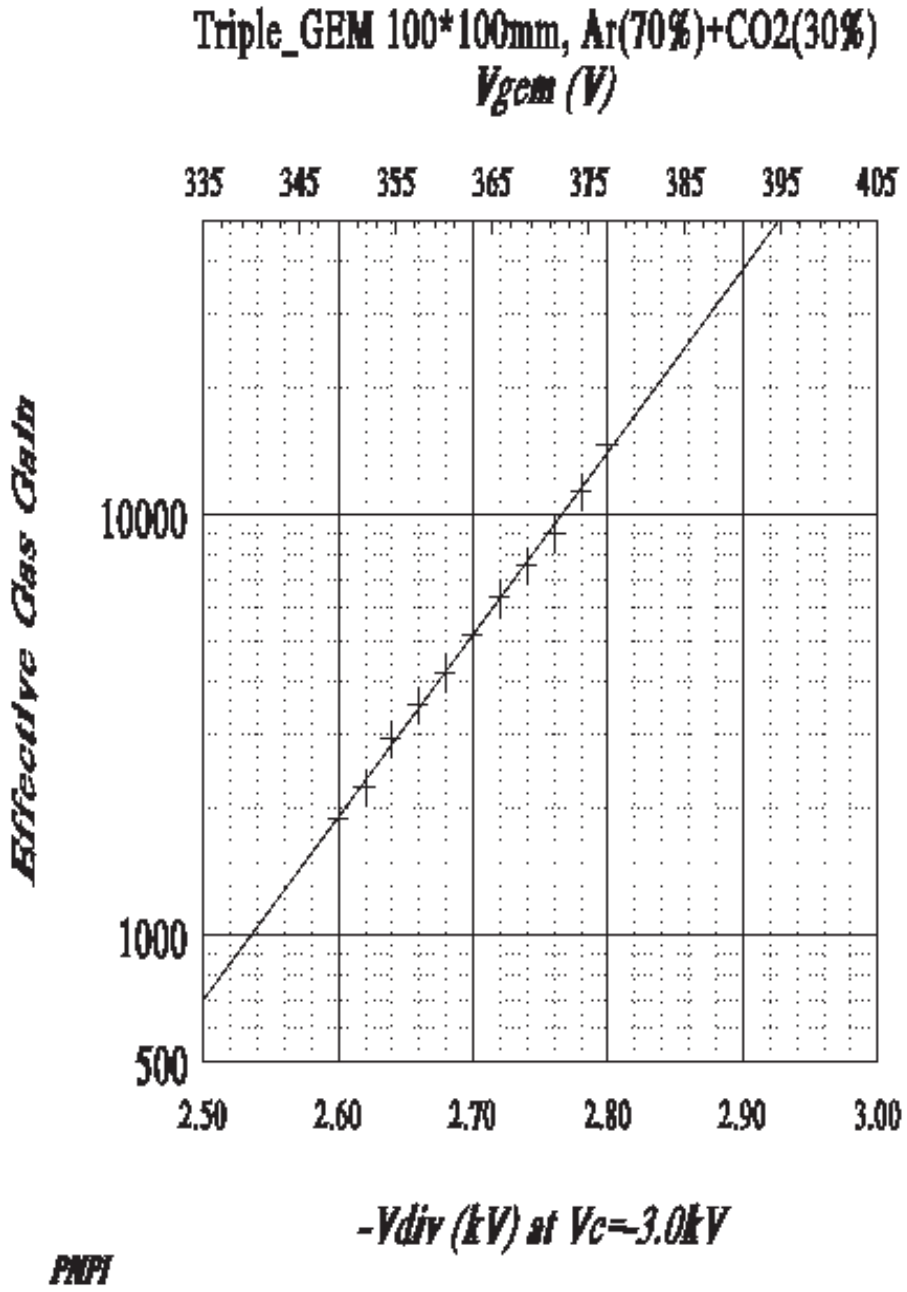

Fig.4. The effective gas gain of the Triple–GEM detector at various V2 (or ΔV_{gem}) and fixed V1=-3.0kV.

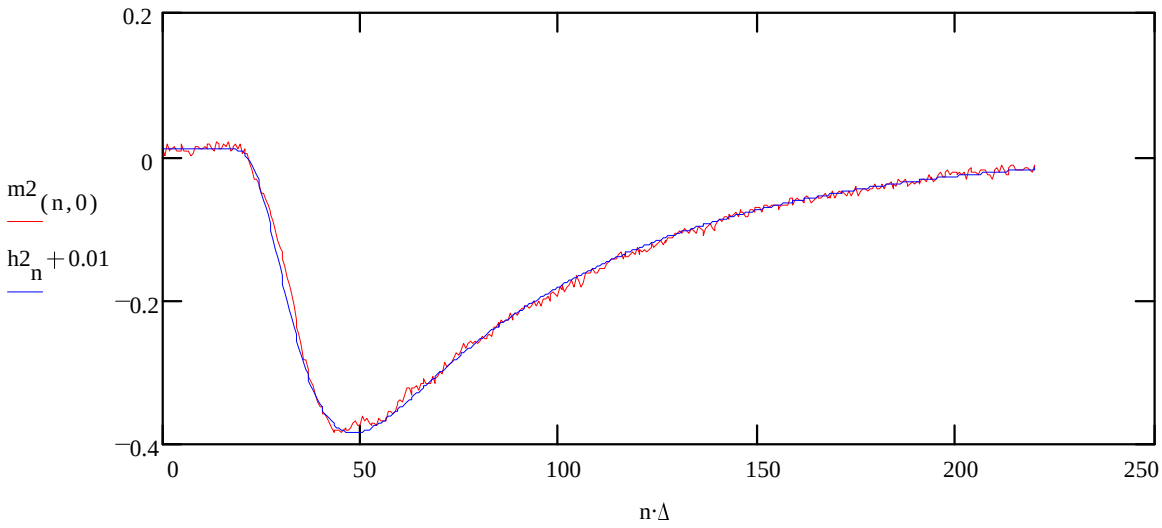

Fig.5. The pulse response of the Common Channel Amplifier
measured by the digital scope and fitted with the function h2c(t). C_{det}≈40pF.

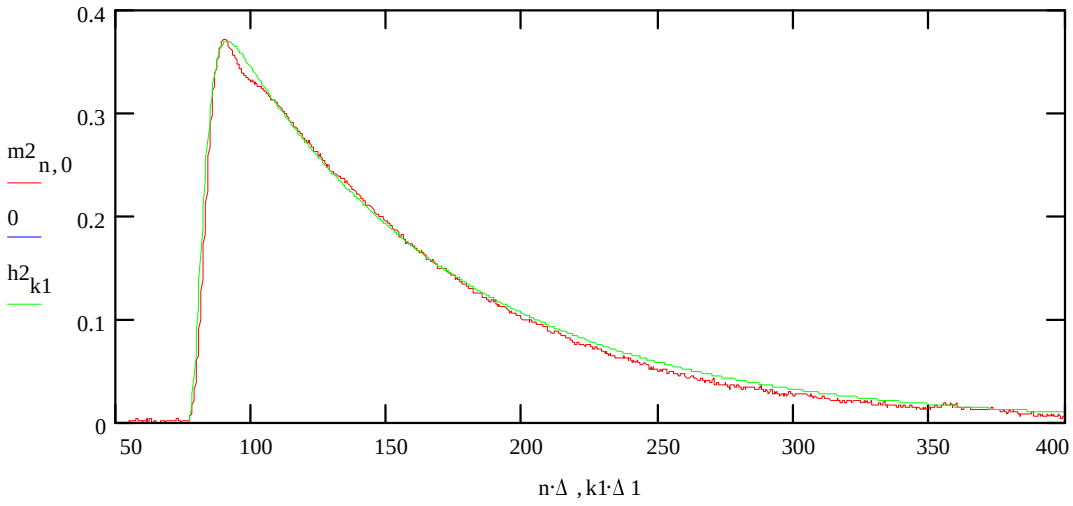

Fig.6. The pulse response of the Strip Amplifier
measured by the digital scope and fitted with the function h2s(t). C_{det}=C_{strip}.

a)

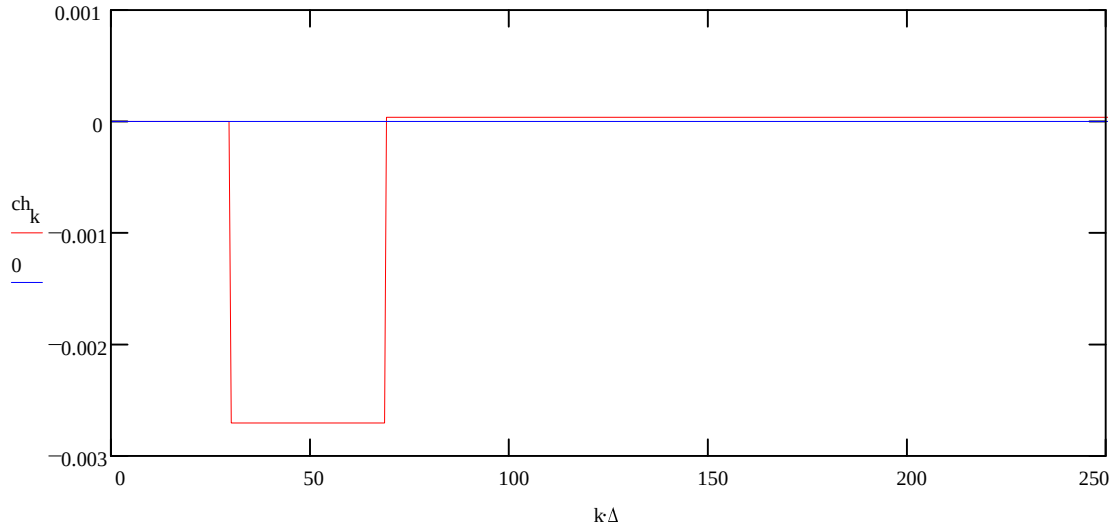

(b)

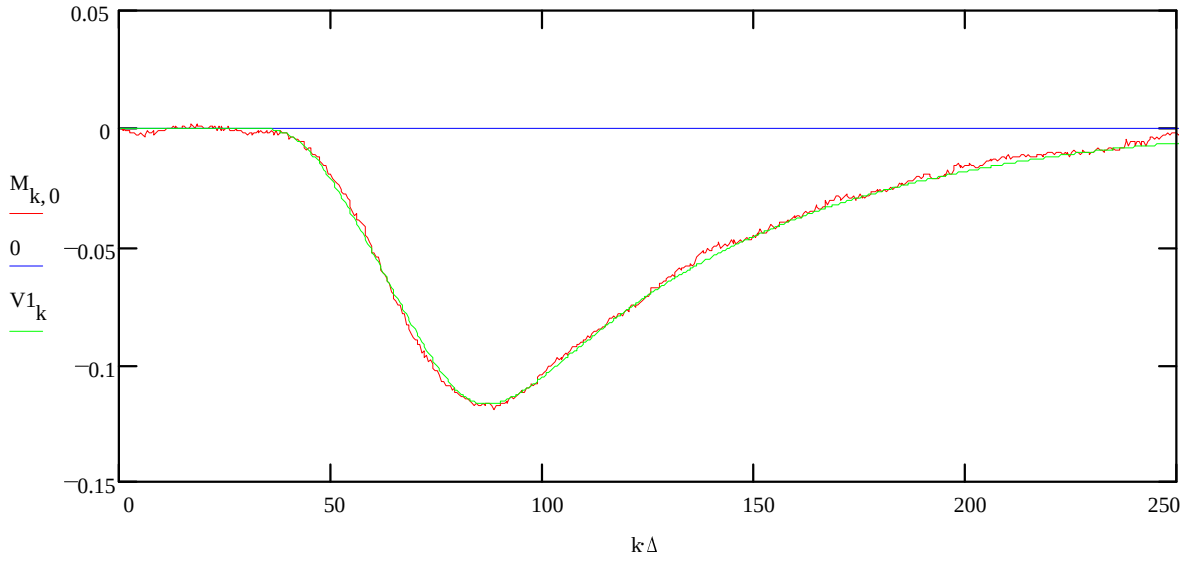

Fig.7. The reconstructed current in the Common Channel *(a)* obtained by the deconvolution of the digital scope signal *(b)*.
(Arbitrary units; time scale in ns).

(a)

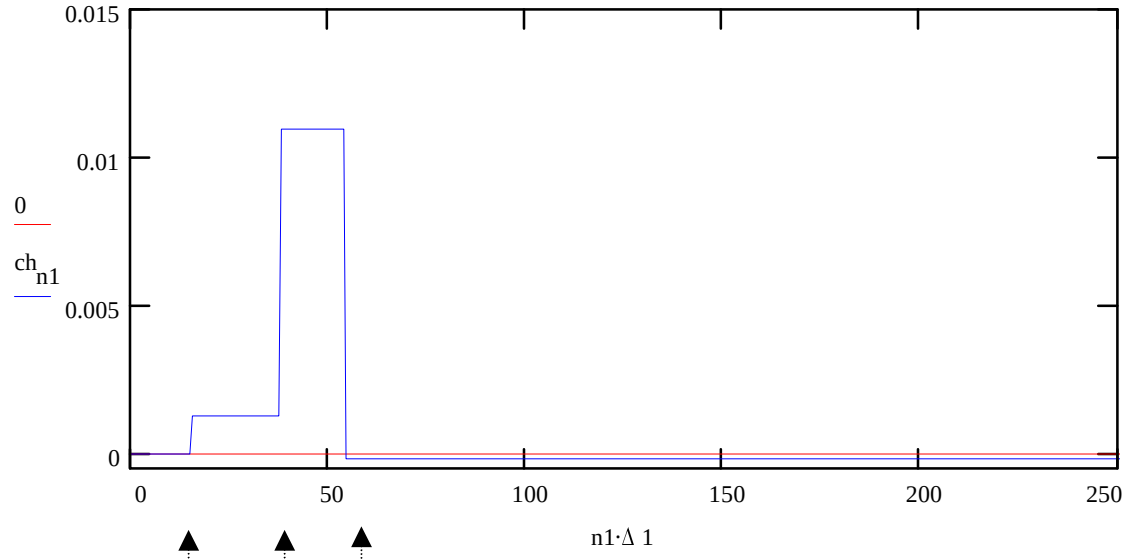

(b)

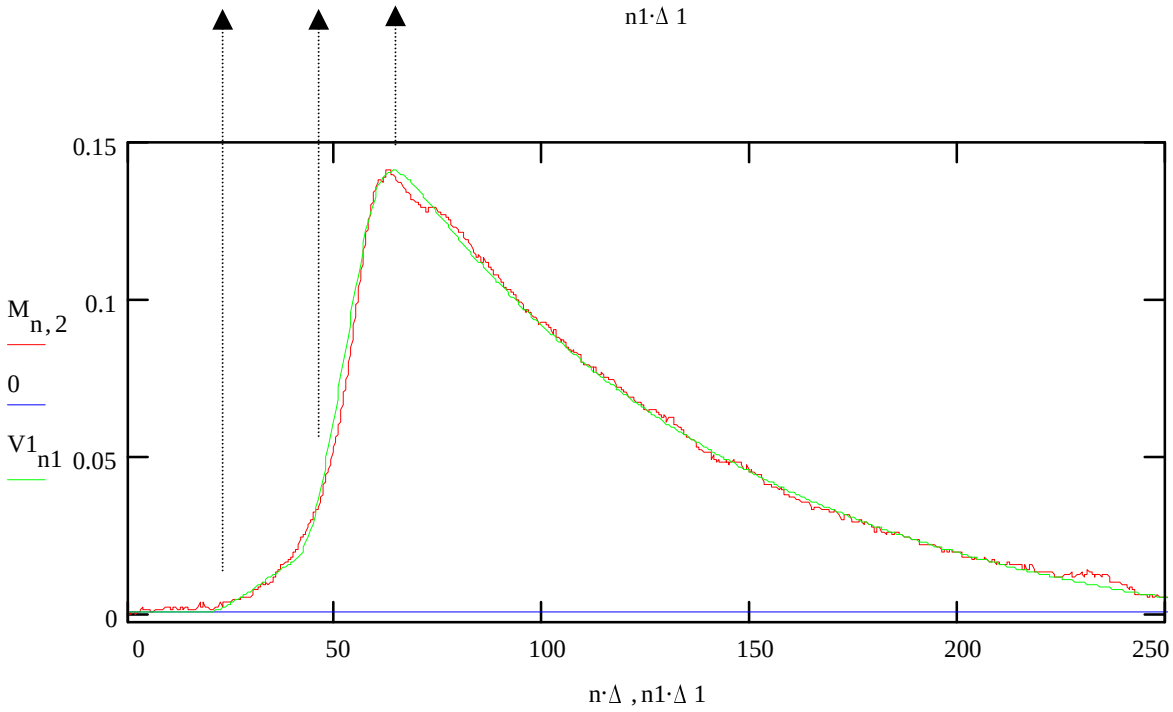

Fig.8. The reconstructed current in the central strip *(a)*
obtained by the deconvolution of the digital scope signal *(b)*.
(Arbitrary units; time scale in ns).

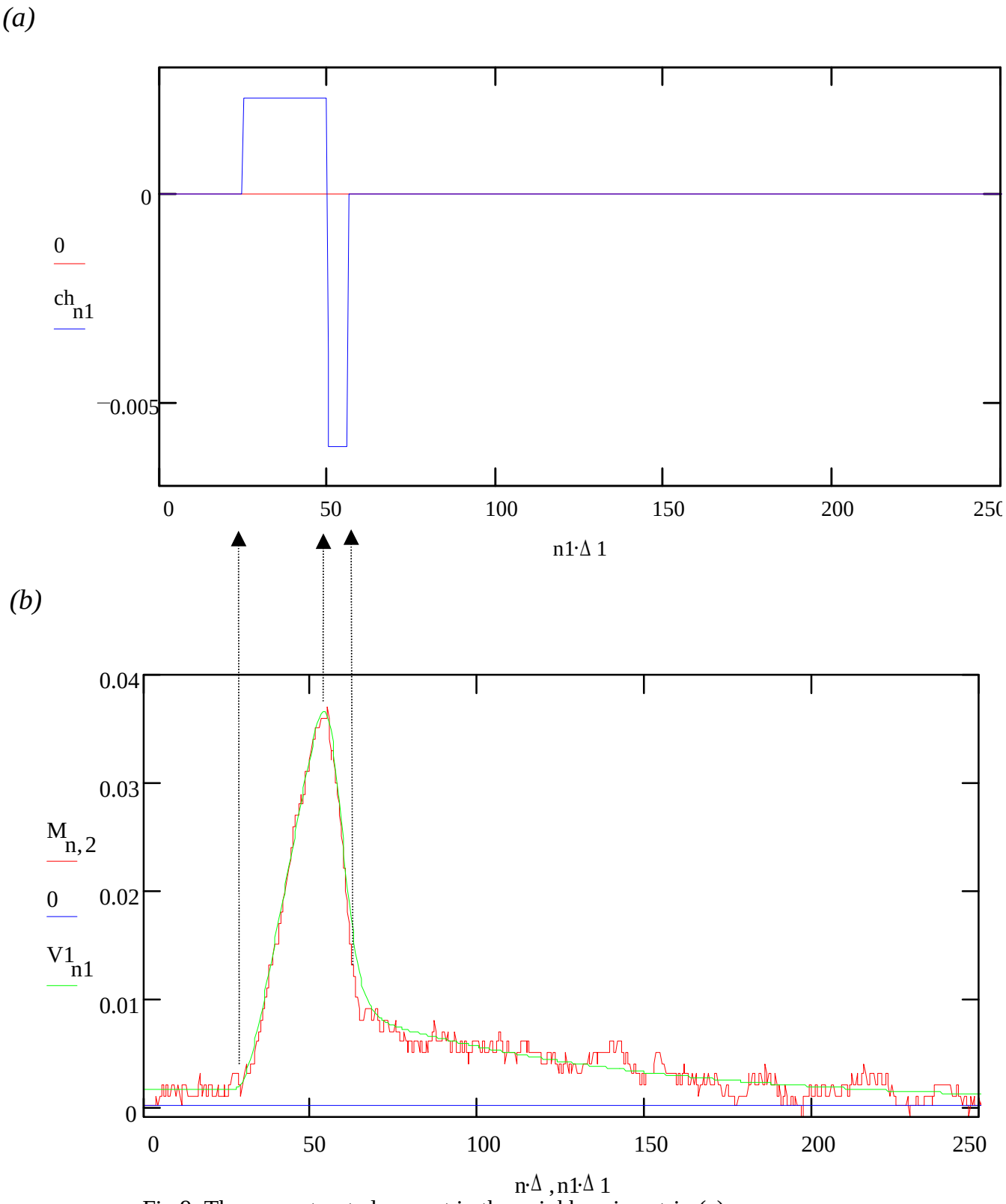

Fig.9. The reconstructed current in the neighbouring strip (a) obtained by the deconvolution of the digital scope signal (b).
(Arbitrary units; time scale in ns).

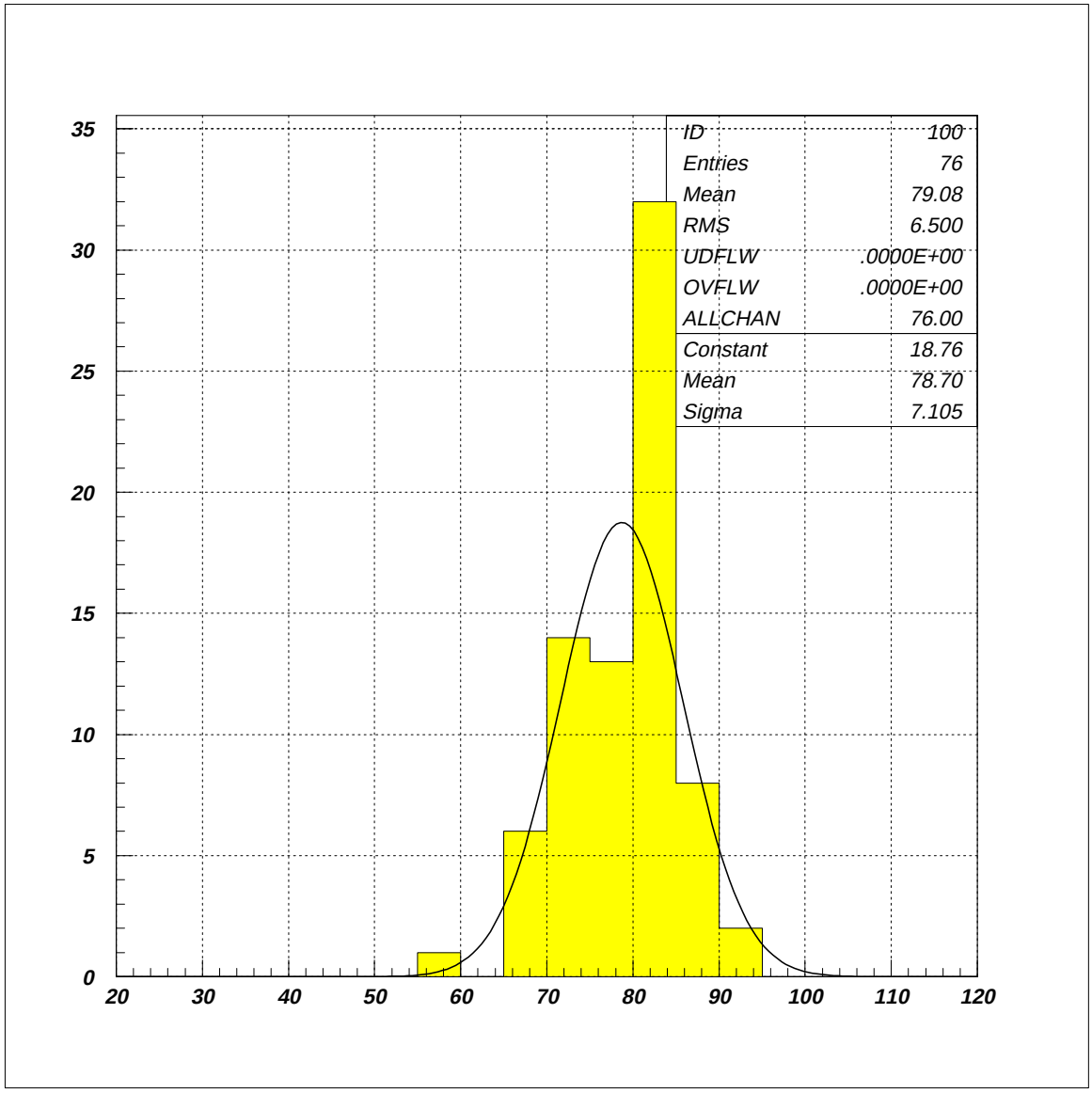

Fig.10. The time resolution of the Triple-GEM detector obtained from the signals recorded in the PSI test run.
The histogram shows a time distribution of the peaking time of signals induced on the central strip (scale in ns).

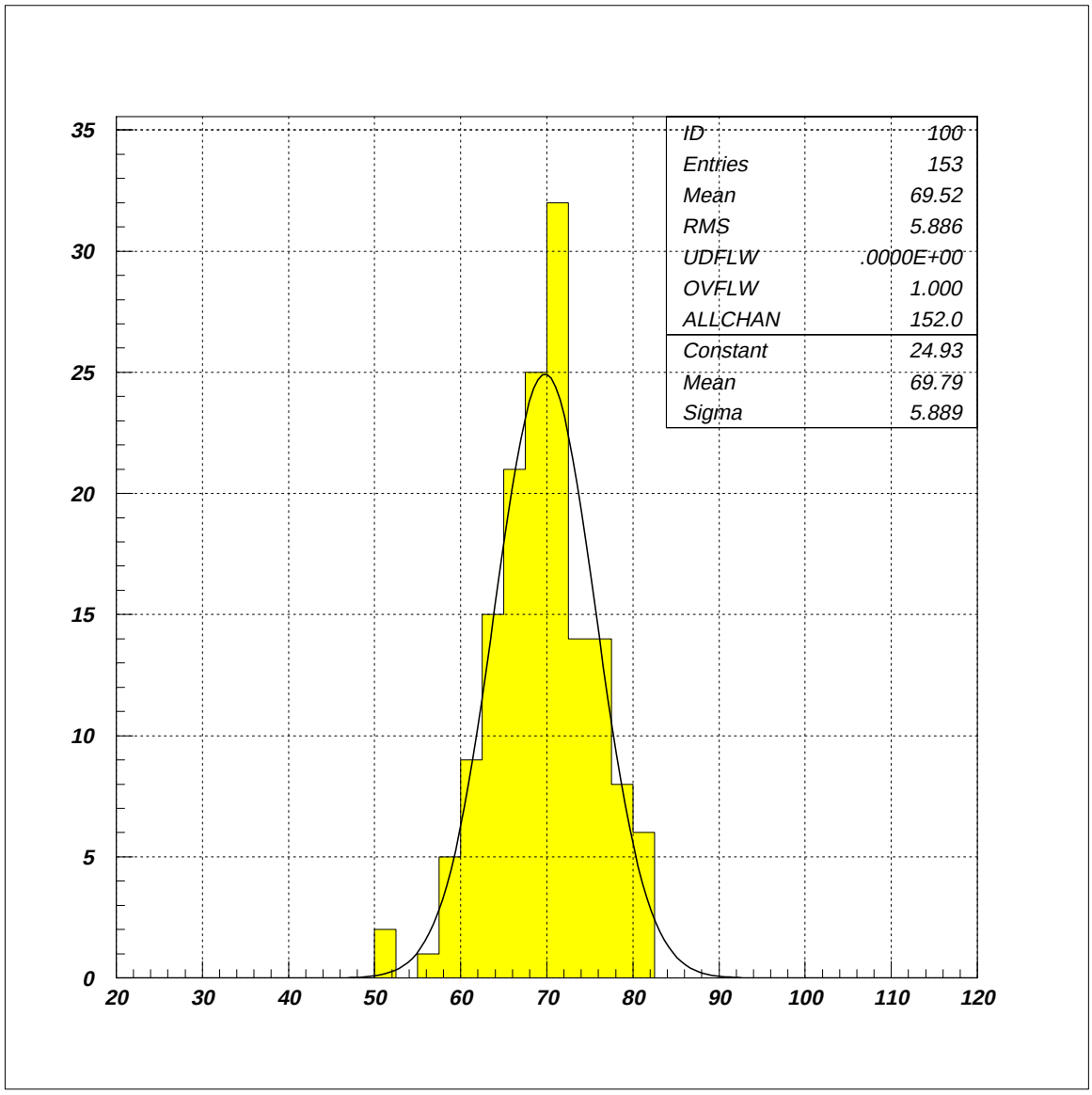

Fig.11. The time resolution of the Triple-GEM detector obtained from the signals recorded in the PSI test run.
The histogram shows a time distribution of the signals induced on the GEM3 (scale in ns).